Therapeutic potential of salinomycin loaded on albumin nanoparticles on cancer stem cells of experimentally induced oral squamous cell carcinoma

Abd El-Hamied Salah Eldin El-Zarka[1], Amr Saad Abd Alwahab [2], Emad Alqalshy[3], Mohamed Mahmoud Ahmed [4]

[1] Assistant Lecturer, Oral, and Dental Pathology Department, Faculty of Dental Medicine (Boys-Cairo), Al-Azhar University, Egypt.

[2] Assistant Professor, Oral and Dental Pathology Department, Faculty of Dental Medicine (Boys-Cairo), Al-Azhar University, Egypt.

[3] Assistant Professor Department of Oral and Dental Pathology, Faculty of Dental Medicine (Boys-Cairo), Al-Azhar University, Egypt

[4] Professor, Oral and Dental Pathology Department, Faculty of Dental Medicine (Boys-Cairo), Al-Azhar University, Egypt.

***** Correspondence: **Abd El-Hamied Salah Eldin El-Zarka**

Email: drabdoo88@gmail.com

Received: 29-6-2023 **Accepted: 30-7-2023** **Published:31-7-2023**

ABSTRACT

Purpose: This study aimed to determine the therapeutic potential of salinomycin (SLA) loaded on albumin nanoparticles on cancer stem cells (CSC) of experimentally induced hamster buccal pouch (HBP) carcinoma.

Material and methods: Thirty Syrian male hamsters were classified into three equal groups (s) (G(s)) of ten each. GI: The animals remained untreated to act as negative controls. The right pouches of animals in GII and GIII were painted three times a week for 14 weeks with 7,12-dimethylbenz (a) anthracene (DMBA). In GII: No additional treatment was administered. While the animals in GIII, were injected intraperitoneal with nano-albumin-bounded salinomycin (NAB-SAL) (5 mg /kg) once every 3 days for 10 times. After the termination of the experiment, gross observations were recorded. Then, the animals were euthanized, all pouches were surgically excised, fixed, and processed for hematoxylin and eosin (H&E) stain examination and immunohistochemical (IHC) staining utilizing (BCL2) as an anti-apoptotic marker and (CD44) as CSCs marker.

Results: In this research, outcomes discovered some variability across medicated G (GIII)contrasted to GII. IHC of both BCL2 and CD44 have highly revealed variation among GI & GII as well as GII & GIII (p-value < 0.001).

Conclusion: NAB-SLA makes an important and useful contribution that inhibits tumor progression through direct influence on CSCs of DMBA-induced HBP carcinoma.

Keywords: HBP carcinoma, albumin nanoparticles, salinomycin, apoptosis, CSCs.

DOI: 10.48047/ecb/2023.12.9.241

1. Introduction:

Oral cancer is one of the most prevalent forms of cancer worldwide. Oral squamous cell carcinoma (OSCC) is a common malignant tumor of the head and neck, and it accounts for more than 90% of oral cancer(1). Valuable knowledge about carcinogenesis has been developed throughout experimental research on animal models. Accumulated evidence pointed out the successful results

when utilizing histological, biochemical, immunohistochemical, and molecular investigations on (DMBA) induced hamster buccal pouch (HBP) carcinoma[(2)].

Conventional treatment strategies, such as surgery, radio, and chemotherapy, have improved over the past few decades; however, they remain far from optimal. Currently, nanotechnology is focused on improving cancer diagnosis and treatment methods. The nanotechnology-based drug delivery systems (DDS) have been heavily investigated in the past few years, to increase the effectiveness of treatment and reduce side effects [(3)].

One of the most important new concepts in stem cell biology is the tumor-initiating cells (TICs) or CSCs which have the ability to differentiate, self-regenerate, and be highly tumorigenic, compared to the other cancer cells and are believed to be largely responsible for the biological characteristics of cancer due to their rapid differentiation, thereby causing tumor formation, progression, invasion, metastasis, and resistance to Conventional treatment strategies [(4)].

Antibiotics are increasingly being used to assist in the treatment of cancers Given the double-edged sword of antibiotics in the development of cancer therapy[(5)]. Various antibiotics have been used in the treatment of cancers, via their anti-proliferative, pro-apoptotic and anti-epithelial-mesenchymal-transition (EMT) capabilities[(6)]. In this case, it seems that the optimal plan to confront cancer is to kill the cancer cells and the CSCs at the same time. Salinomycin (SAL), was an antibiotic isolated from streptomyces albus, which show a broad spectrum of bioactivity, including antibacterial, antiparasitic, antifungal, antiviral activity SAL as an effective agent against CSCs which overcomes drug resistance in human cancer by suppress CSCs proliferation and inducing apoptosis[(7)].

SAL loaded nanoparticles resulted in specific targeting of CSCs through CD44 interactions SAL mediates its anticancer effect by various mechanisms in different cancer types which shows cytotoxic effect by disrupting the balance of sodium and potassium ions across the cell membrane and the mitochondrial membrane, Rapid efflux of K+ from cell mem -brane and mitochondrial membrane led to apoptosis of cells[(8)] .

SAL inhibited mitochondrial oxidative phosphorylation without affecting the substrate-level phosphorylation. SAL triggers apoptotic cascade, independent of the cell-cycle arrest, p53, and proteasome .SAL induced apoptosis even in those cells which acquire resistance to the apoptosis by higher expression of anti-apoptotic protein Bcl-2, or 26 proteasomes[(9)], It induced oxidative stress and finally reduced CD44 cell population, SAL increased tumor-suppressor protein p53 and DNA damaging protein pH2AX and decreased cyclin D1 level ,which led to cell-cycle arrest and high DNA damage[(10)]. In Head and neck cancer Induces cell death and decreases CD44+ population in JLO-1 and UMSSC-10B in head and neck squamous cell carcinoma in vitro[(11)].

Apoptosis, or programmed cell death, was found to play a pivotal role in the regulation of OSCC[(12)]. Many signals for cellular life and death are regulated by the BCL-2 family proteins and converge at mitochondria, where cell fate is ultimately decided, Since BCL-2 is one of anti-apoptotic proteins, they are expected to function as oncogenes in cancer cells, cancers over-expressing Bcl-2 should have worse prognosis. However, studies analyzing the prognostic significance of apoptotic proteins in OSCC have yielded contradictory results[(13)].

Many researchers have been trying to achieve a "magic bullet" concept in drug delivery systems. especially nanocarriers that will particularly target actives to cancerous tissue. It has been reported that the expression of several proteins is associated with CSCs features. CSC markers are unique in the case of tumor and/or phenotype and require biological confirmation to the anticipated phenotype[(14)]. In cancer therapy, molecularly targeted agents have the potential to maximize

antitumor efficacy while minimizing treatment-related toxicity, A potential biological target is the folate receptor (FR), which has been shown to be overexpressed on the surface of many cancers, including tumors of the lungs and ovaries[15].

Thus, the primary aim of this study was to determine the efficacy of NABs-SAL as a new paradigm on cancer stem cells of DMBA induced HBP carcinoma. The evaluation depends on the animal's general health examinations, HBP gross observations, histological tumor tissue changes and immunohistochemistry (IHC) examinations.

2. Material and Methods

2.1 Chemicals

DMBA (0.5%) was gathered from Sigma-Aldrich company, solubilized in paraffin oil.

SAL (Sigma-Aldrich company, USA) was prepared by Dissolved in0.9% sodium chloride (10 mg/ml).

2.2 Animals

Thirty Syrian male hamsters, weighing between 80 and 120g, and five weeks old. The experimental hamsters were kept in standard boxes with sawdust bedding in a controlled environment with humidity (30-40%), temperature (20 ±2°C), and light (12-hour light/12-hour dark). A healthy hamster walked regularly and smoothly, had bright, clear eyes, healthy skin, and a soft, lustrous coat devoid of parasites, wounds, dry spots, and swellings.

Ethical Approval

Ethical approval cleared by ethical committee of Faculty of Dental Medicine (Boys- Cairo), Al-Azhar University, Egypt (Ethical Code No. 411/1942).

2.3 Experimental design

Three groups (Gs) of ten animals each had been created at random from animals. following week of adjustment. While animals in GI (negative control) had been left untreated, the right pouches of animals in GII and GIII had been painted 3times per week for fourteen weeks with 0.5 percent DMBA in liquid paraffin. animals in GII (positive control) did not get further treatment after that, but those in GIII (NAB- SAL) did so following completion of 14-week DMBA painting experiment[16] . NAB-SAL will be administrated intraperitoneally IP (5 mg /kg) once every 3 days for 10 times times[17]. Then they were euthanized after 3 weeks follow up.

2.4 General health examinations

The alterations in the animal's general health were monitored throughout the experiment. Hamsters that demonstrated any of the following signs (crowding in sneezing, anorexia, silence, corner, diarrhea, discharge from the nose or eyes, dampness around the tail, wheezing, and hair loss) of illness or disease were adapted[18].

2.5 Tumor volume measurement

After termination of the experiment, gross observations of HBP mucosa were recorded (mucosal thickness, exudation, ulcers, and tumors). Then, the animals were euthanized, the right cheek pouch everted, and the diameter of each tumor was measured with a Vernier calliper. The tumor volume, where the three diameters (mm) of the tumor are D1, D2 and D3, was calculated by the formula, $Vmm3 = (4/3)\ \pi\ [(D1/2)\ (D2/2)\ (D3/2)]$ [18].

2.6 Sample collection and preparation

The right cheek pouch was excised, fixed in 10% neutral buffered formalin, routinely processed, and embedded in paraffin blocks to be examined histologically and IHC utilizing BCL-2 and CD44.

2.7 **Histopathological examinations**

Utilizing a rotary microtome, 4 **µm** thick tissue sections were cut from paraffin blocks, processed, mounted on glass slides, and stained with Hematoxylin and Eosin (H&E) for light microscopic inspection.

2.8 **Measurement of the depth of invasion (DOI)**

The DOI of all surgical specimens was determined using the H&E slide. The DOI was calculated from the surface epithelium's basal layer to the deepest point of tumor infiltration. According to the American joint committee of cancer (AJCC), it is further characterized as less invasive at ≤5 mm, moderately invasive at 6-10 mm, and highly invasive at ≥10 mm [19] **(Fig.1)**. The DOI was determined by a Leica QWIN V3 image analyzer computer system (Switzerland), which was operated via the Leica QWIN V3 software. This was done in Oral and Dental Pathology Department, Faculty of Dental Medicine (Boys-Cairo), Al-Azhar University, Egypt.

2.9 **Immunohistochemical examination** [20]

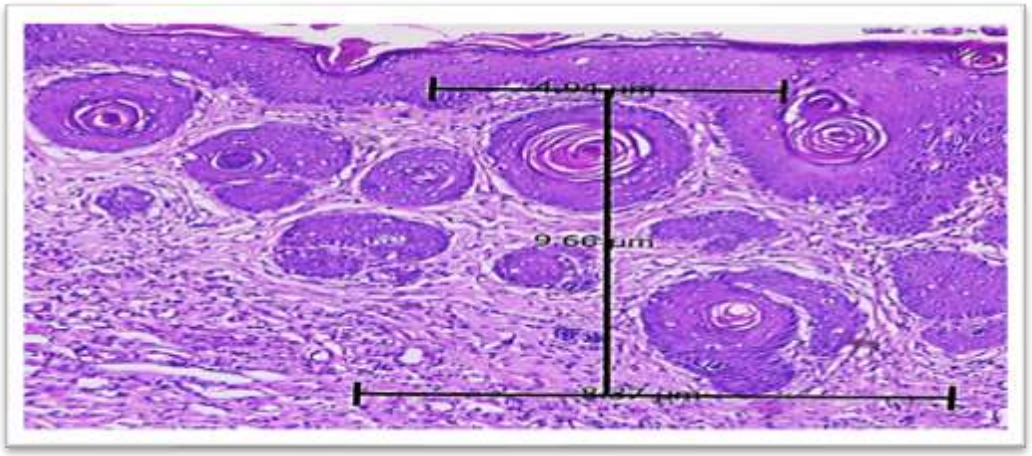

Fig. (1): Photograph of measuring the DOI, the greatest invasion was measured by dropping a "plumb line" from the horizon to the deepest invasive nest.

For IHC staining, streptavidin biotin peroxidase (SBP) method, the following steps were performed according to manufacture instructions: Paraffin blocks were cut into 5µm thick sections and mounted on positively charged glass slides. Each specimen was carried into two similar slides, one for BCL2 and one for CD44 antibody.

I-BCL2: Positive control: To specify the bcl2 antibody as data sheet recommended, tissue sections of tonsillar tissue were stained and examined. Tissue sections revealed positive cytoplasmic brown staining **(Fig.2, A), Negative control:** The primary antibody phase was skipped, and staining process continued **(Fig.2, B). II-CD44: Positive control:** To specify the CD44 antibody as data sheet recommended, tissue sections of spleen tissue were stained and examined. Tissue sections revealed positive membranous yellowish staining **(Fig .2, C), Negative control:** The primary antibody phase was skipped, and staining process continued **(Fig.2, D).**

The immunostained sections were examined using light microscope to assess the prevalence of positive cases and the localization of immunostaining within the tissues. In addition, image analysis computer system was used to assess area percentage of positive cells of the

immunostaining. This was done in Oral and Dental Pathology Department, Faculty of Dental Medicine (Boys-Cairo), Al-Azhar University, Egypt.

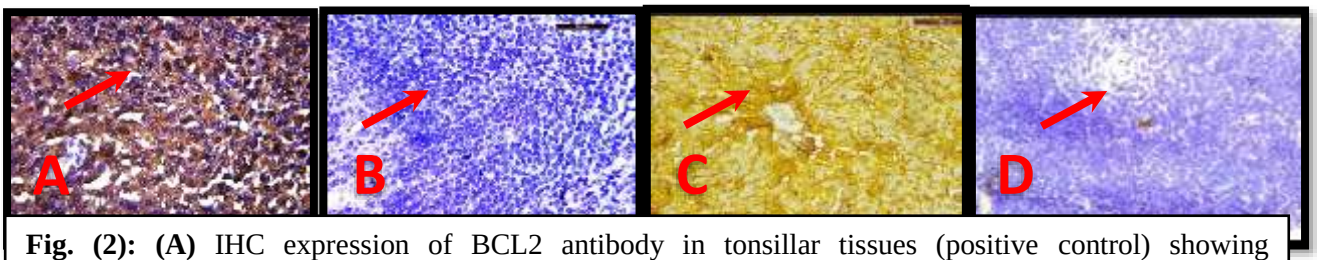

Fig. (2): (A) IHC expression of BCL2 antibody in tonsillar tissues (positive control) showing positive cytoplasmic staining (arrow) **(X400). (B)** The tonsillar tissues (negative control) showing negative expression (arrow) **(X400). (C)** IHC expression of CD44 antibody in spleen tissues (positive control) showing positive membranous staining (arrow) (X400). **(D)** The liver tissues (negative control) showing negative expression (arrow) (X400).

2.10 Statistical analysis

The data were statistically examined, and the mean and standard deviation were calculated (SD). A one-way analysis of variance was performed using SPSS version 17.0 for Windows (ANOVA). With quantitative data and parametric distribution, ANOVA was utilized to differentiate between more than two separate groups, accompanied by post hoc analysis with the LSD test. To establish significance, the relevant p-values were used: p 0.05: significant, p > 0.05: non-significant, and p< 0.001: extremely significant.

3 Results

3.1 Gross observations

GI examination revealed no obvious alterations, neither hair loss nor skin ulcerations. The HBP was normal pale pink with no pathological or inflammatory signs **(Fig. 3 A)**. In **GII**, all hamsters demonstrated debilitation and observable hair loss with para-oral skin ulcerations. The right HBP mucosa showed multiple exophytic variable size nodules with roughened granular surface. The nodules were surrounded with ulcerative and bleeding areas. **(Fig. 3 B)**. The mean tumors volume measurement of tumor-bearing animals in ten animals in **GII** was 773.99 mm3 (620 – 1005 mm3**(Table.1).**). In **GIII,** all hamsters showed slight improvement in general health compared to the animals in GII. The right HBP mucosa showed various changes, multiple exophytic masses of small sizes surrounded with areas of ulceration and bleeding (6 hamsters out of 10), and small exophytic

(Fig.3A): Photograph of GI showing normal buccal pouch mucosa which appeared pink in color with smooth surface (arrow). **(Fig.3B):** Photograph of GII showing multiple exophytic papillary tumor masses surrounded with bleeding areas (arrows). **(Fig.3C):** Photograph of GIII showing multiple exophytic small size nodules surrounded with area of bleeding (arrow).

nodule with absence of ulceration and bleeding (4 hamsters out of 10) **(Fig.3 C)**. There was a decrease in the mean tumor volume of GIII (493.11 mm3) compared to that of GII**(Table.1**).

3.2. Statistical analysis results of tumor volume:

Regarding **tumor volume**, there had been greatly variation (p value < 0.001) among GII & (GIII)**. (Table. 1 & Chart. 1).**

A	Tumor volume		P-value for post analysis usingLSD test	
	Mean ± SD	Range	GII	GIII
GII	773.99±56.27	693.2– 860.4	--	0.000
GIII	493.11±40.49	443.7– 588.4	0.000	--
F	579.257			
P-value	<0.001 (HS)			

Table (1): Comparing studied groups as regard to tumor volume.

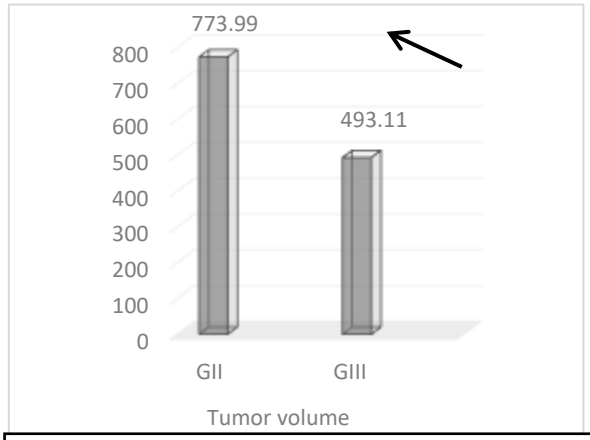

Chart. (1): Comparing studied groups regarding tumor volume level.

ngs reve xhib cells and one, two or three layers of spinous and thin keratinized cells with lacking rete ridges. Sub epithelial CT, muscular layer and areolar layer were seen **(Fig.4A)**. The IHC staining using Bcl-2 exhibited positive cytoplasmic expression (mean = 6.87) **(Table.3),** which limited to basal and suprabasal layers **(Fig.4B)**. The IHC staining using **CD44** antibody exhibited positive membranous expression (mean = 34.98 %) **(Table.4)** which limited to basal and suprabasal epithelial layers **(Fig.4C).**

GII: Histological sections, using H&E stain, revealed variable changes. In 7 hamsters out of 10 exhibited well differentiated SCC and, the other 3 hamsters exhibited moderate SCC. The overlying epithelium revealed multiple areas with dysplastic features consisting of pleomorphic, hyperchromatic nuclei exhibited altered nuclear/cytoplasmic ratio and exhibited destruction of the basement membrane. well differentiated SCC with true invasion of malignant cells which appeared as epithelial pearls with keratin foci or cell nests or in the form of detached and scattered cell with evidence of keratin formation. moderately differentiated SCC was composed of cords or islands of neoplastic atypical epithelial cells, oval-shaped, round which infiltrated the tumoral stroma with less keratin formation. **(Fig.4D).** The mean DOI revealed 9.68 mm **(Table.2)**. The IHC staining using Bcl-2 exhibited positive cytoplasmic expression (mean = 70.83) **(Table.3)** throughout the epithelial layers and invading tumor cells **(Fig.4E).** The IHC staining using **CD44** antibody exhibited positive membranous-cytoplasmic expression (mean= 66.18 %) **(Table.4)** throughout the epithelial layers and invading tumor cells **(Fig. 4F).**

GIII: Histological sections, using H&E stain, revealed variable changes. In 6 hamsters out of 10, exhibited different degrees of epithelial dysplasia, 3 out of 6 hamsters revealed moderate dysplasia, and the other 3 hamsters revealed sever dysplasia which extending more than two-thirds of the epithelial thickness. above an intact basement membrane. In the other 4 hamsters, the dysplastic overlying epithelium was accompanied by destruction of the basement membrane. The underlying CT showed superficial invasion of the dysplastic epithelial cell nests and keratin pearls in the form

of well differentiated SCC, which was limited to the nodules only, not extended to the deeper areas. There was reduction of the inflammatory infiltration and increase amount of keratin formation and collagen fibers **(Fig. 4G)**. The mean DOI in GIII (10 hamsters) was 3.86 mm **(Table.2)**. The IHC staining using Bcl-2 positive cytoplasmic expression (mean=57.51) **(Table.3)** throughout the epithelial layers and superficial invading tumor cells **(Fig. 4H).** The IHC staining using **CD44** antibody exhibited positive membranous expression (mean= 49.07 %) **(Table.4)** throughout the epithelial layers and invading tumor cells **(Fig. 4I).**

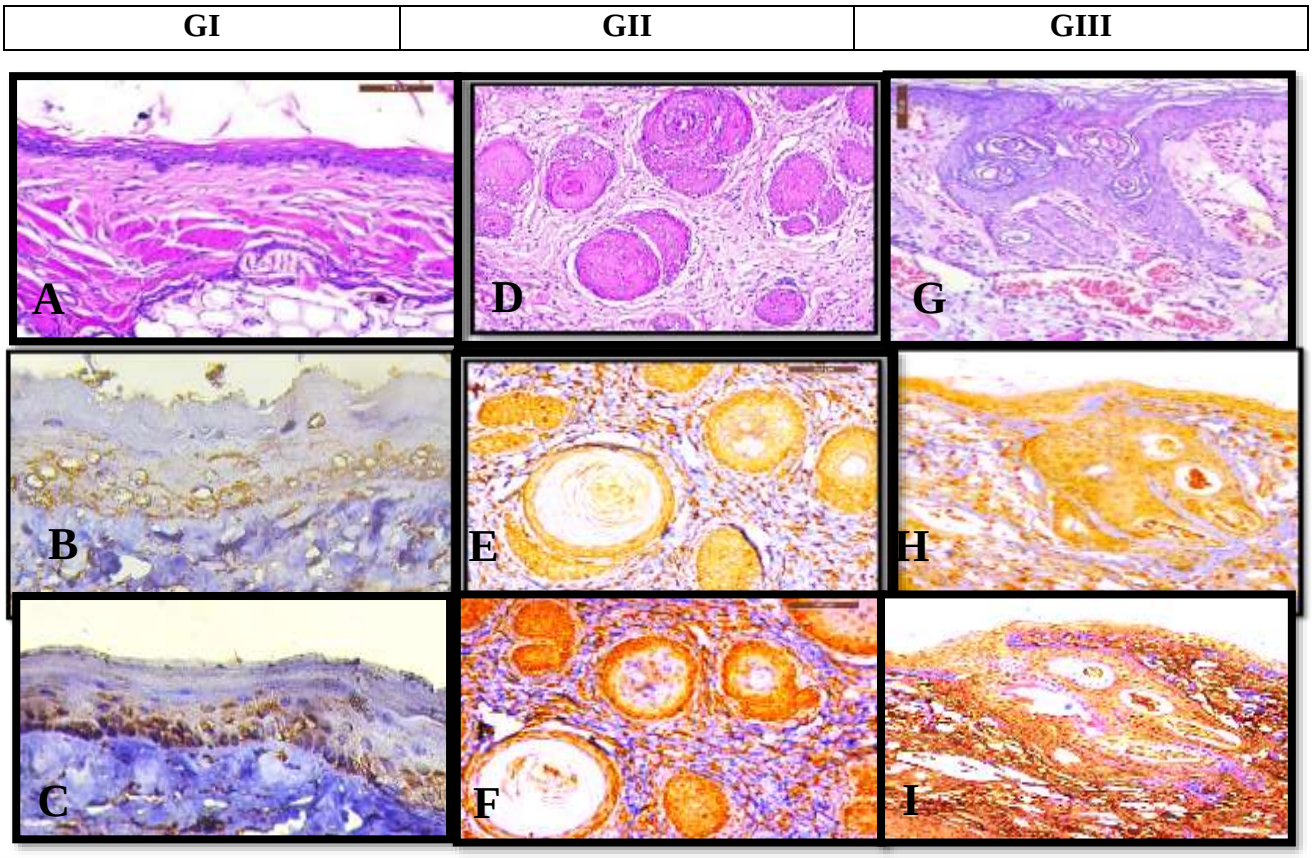

(Fig.4): A- Photomicrograph of GI showing epithelium consists of two to four layers, superficial squamous cells exhibiting keratinization, flattened rete ridges, C.T layer, muscular layer, and deep layer of loose areolar connective tissue (H&E stain X100). **B-** The IHC expression of Bcl-2 of **GI** showing positive cytoplasmic expression in basal and suprabasal epithelial layers. (Streptavidin biotin peroxidase, X 200). **C-**The IHC staining using CD44 antibody exhibited positive membranous expression in almost all normal epithelial cells (Streptavidin biotin peroxidase, X 200). **D-** Photomicrograph of GII showing well differentiated SCC with deep invasion of multiple tumor islands into the underlying connective tissue and sub-epithelial inflammatory infiltrates (H&E stain X200). **E-** The IHC expression of Bcl-2 showing strong positive cytoplasmic expression throughout invading tumor nests. (Streptavidin biotin peroxidase, X 200). **F-**The IHC staining using CD44 antibody exhibited positive membranous expression throughout the epithelial layers and invading tumor cells (Streptavidin biotin peroxidase, X 200)**. G-** Photomicrograph of GIII showing well differentiated SCC (superficial invasion) (H&E stain X100). **H-** The IHC expression of Bcl-2 showing positive cytoplasmic expression throughout the epithelial layers. (Streptavidin biotin peroxidase, X 100). **I-**The IHC staining using CD44 antibody exhibited positive membranous expression throughout the epithelial layers and invading tumor cells (Streptavidin biotin peroxidase, X 100

3.4 Statistical analysis results of DOI:

Regarding DOI, there had been greatly variation (p value < 0.001) among GII & the treated Gs (GIII). **(Table. 2 & Fig.5).**

	DOI		P-value for post analysis usingLSD test	
	Mean ± SD	**Range**	**GII**	**GIII**
GII	9.66 ± 1.79	8.4 – 13.9	--	0.000
GIII	3.86 ± 1.10	2.6 – 5.7	0.000	--
F	**175.607**			
P-value	**<0.001 (HS)**			

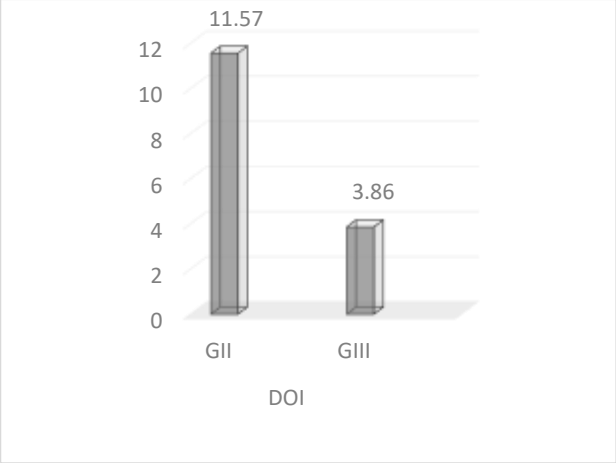

Table (2): Comparing studied groups regarding DOI.

Chart. (2): Comparing studied groups regarding DOI level**.**

3.4 Statistical analysis results of immune staining:

Regarding Bcl-2, mean area % for GI was lowest (6.87%), while mean area % for GII was greatest (70.83%). variation among GI and GII had been highly significant (p value< 0.001). When GII and GIII were compared, there had been highly variation among two (p value <0.001) **(Table. 3 & Chart. 3).**

	Bcl2		P-value for post analysis using LSD test		
	Mean ± SD	**Range**	**G1**	**GII**	**GIII**
G1	6.87 ± 1.50	4.2 – 9.1	--	0.000	0.000
GII	70.83 ± 4.47	63.8 – 76.8	0.000	--	0.000
GIII	57.51 ± 4.31	49.6 – 62.3	0.000	0.000	--
F	**497.581**				
P-value	**<0.001 (HS)**				

Table (3): Comparison among studied groups regarding BCL2 level.

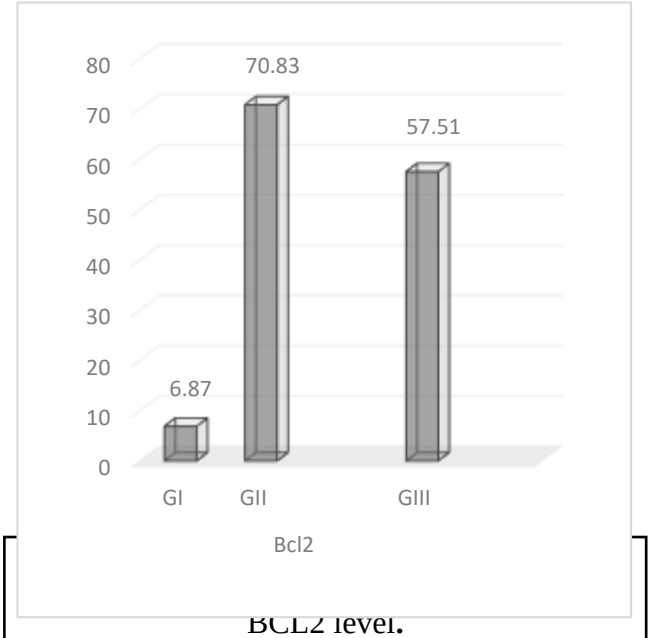

BCL2 level.

Regarding CD44, the mean area % for GI was lowest (34.98%), while mean area % for GII was greatest (66.18%). variation among GI and GII had been highly significant (p value< 0.001). When GII and GIII were compared, there had been highly variation among two (p value <0.001) **(Table. 4 & Chart. 4)**.

	CD44		P-value for post analysis using LSD test		
	Mean ± SD	**Range**	**G1**	**GII**	**GIII**
G1	34.98 ± 2.13	29.8 – 37.4	--	0.000	0.000
GII	66.18 ± 3.03	59.8 – 70.3	0.000	--	0.000
GIII	49.07 ± 2.54	45.3 – 54.1	0.000	0.000	--
F	**51.508**				
P-value	**<0.001 (HS)**				

Table (4): Comparison among studied groups regarding CD44 level.

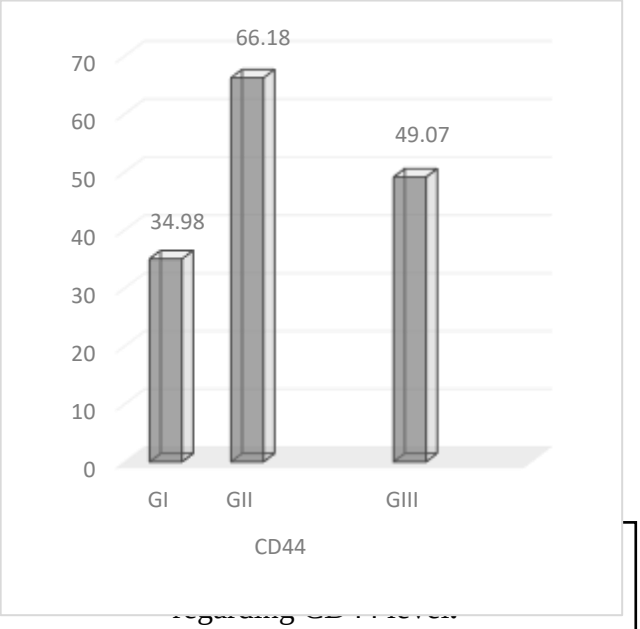

4 Discussion

To address whether the value of NAB-SAL as an effective drug against cancer and CSCs for treatment and inhibition of tumor progression of DMBA induced hamster buccal pouch carcinoma, this study was done.

The CSC population possesses characteristics associated with stem cells, including self-renewal and exhibits high in vivo tumorigenicity and differentiation potential, in addition to apoptotic resistance[21], this was the first study to evaluate the efficacy NAB-SAL on DMBA induced HBP carcinoma. The results of animal's general health examinations, HBP gross observations, H&E stain and IHC examination, revealed variable observations.

In the present study, the gross observation findings in GI didn't show any change, no perioral skin ulcerations, or hair loss. The HBP mucosa showed a normal pale pink color. These results agree with the studies reported the same findings [22]. After sacrificing, this finding reflected on H&E staining which showed normal thin stratified squamous epithelium formed of two to four cell layers, lacking rete ridges and thin keratin surface layer. These results agree with the studies reported by Samah K et al. [23]. These results may be due to the hamsters not being exposed to the carcinogenic agent.

.

In the current study, The IHC results of Bcl-2 in G1I showed positive expression (mean = 6.7) which limited to basal and suprabasal layers. This result may be due to bcl-2 participating in the control of the terminal differentiation of keratinocytes by protecting their stem cells from apoptosis. The finding of this study was in agreement of some researches[24, 25]. Singh n et al**. [26]** stated that, under normal conditions, Bcl-2 ratio determines the fate of cell survival or cell death, through the regulation of the release of Cyt C from the mitochondria.

The IHC staining of CD44 in GI showed positive membranous expression (mean = 35.3%) in the basal and parabasal cells with negative expression in the corneal and subcorneal layers, Kaza et al., showed that the positive expression of CD44 observed in the generative cells of the epithelium implicate that these cells could be the targets for malignant transformation[27]. This result is in agreement with that of other investigators [28, 29] .

In the current study, the gross observation findings in GII showed general debilitation of animals, perioral hair loss, and skin lesions, the HBP showed multiple exophytic variable size nodules surrounded by area of ulceration and bleeding. The mean tumor volume of the tumor-bearing animals was 773.99 mm^3 . These observations are mainly due to the strong toxic DMBA effect. This result agrees with another investigator[23, 30]. This finding reflected on H&E staining in which DMBA-induced HBP tumors were found various patterns of invasive OSCC (70% well differentiated and 30% moderately differentiated) in the form of dysplastic lesions with deeper invading islands of epithelium into underlying connective tissues (DOI=9.66 mm) . These results in consistence with that shown by other researchers[31, 32]. These findings may be referred to higher level of intracellular ROS during DMBA application which results in chronic oxidative stress[33]. Furthermore, ROS has been implicated in all the three stages (initiation, promotion, and progression) of carcinogenesis. Overproduction of ROS in the body causes extensive DNA damage that could in turn contribute to neoplastic transformation. ROS-mediated DNA damage could cause structural modifications in DNA, activation of proto-oncogene, and inactivation of tumor suppressor genes, which eventually leads to neoplastic transformation[34].

In the current study, IHC staining of GII showed positive cytoplasmic expression of BCL2 (70.85 %) **,** that was seen throughout the epithelial layers and invading tumor cells, that showed highly significantly expression compared to GI (p value < 0.001) These results are in agreement with those of some studies[35-37] Over expression of anti-apoptotic Bcl-2 may contribute to that, Bcl-2 prolong cell survival through inhibiting apoptosis by prevent the release of Cyt C from mitochondria and may promote tumor development, Chen Yu *et al* [36]concluded that the cells located within infiltrating tumor nests were more intensely stained in OSCC cases. Similar results were observed by other investigators[38, 39].

The IHC staining of CD44 in GII showed positive membranous expression of (mean=66.18 %) **(**that was seen throughout the epithelial layers and invading tumor cells, that showed highly significantly expression compared to GI (p value < 0.001). In agreement with the present study results, Mirhashemi M et al, showed that higher expression of CD44 was reported in the OSCC with higher grade and stage [40]. Similar to the present study, the results of Tanushree K. et al[41], Tetsuya T. et al[42], confirmed that increased expression of CD44 would increase the risk of malignancy. Paulis et al[43] concluded that, CD44 expression increased the aggressiveness of tumor cells behavior. On the other hand, Margaritescu et al[44] showed a limited usefulness of CD44 expression in identifying the CSCs in OSCCs.

In the present work, GIII showed relatively slight improvement in the animal's general health compared to the animals in GII. The right HBP mucosa showed a relative decrease in size of exophytic nodules. There was a decrease in the mean tumor volume (493.11 mm3) compared to that of GII. These findings conflicted on H&E staining in which six out of 10 hamsters revealed different degrees of epithelial dysplasia {(moderate (3), severe (3)}, while the other four hamsters showed well differentiated SCC with superficial invasion of the malignant cells to the underlying CT which was limited to the nodules only, not extended to the deeper areas. There was a reduction of inflammatory infiltration and an increase in the amount of keratin formation and collagen fibers. The mean DOI was (3.86 mm) that was decreased compared to GII with high significantly difference expression compared to GII (p-value = 0.001). These results are in agreement with Paik et al[45] whom reported that, the tumor volume of the NAB-SAL had significantly decreased by 50% compared with controls. Daily monitoring of animals throughout the therapy showed acceptable tolerability with no unfavorable side effects such as changes in body weight, mobility, posture, or feeding habits.

The IHC staining of GIII using Bcl-2 positive cytoplasmic expression (mean=57.51) throughout the epithelial layers and superficial invading tumor cells which revealed that OSCC treatment with NAB-SAL displayed higher apoptosis than GII with high significance difference (p value <0.001). These results are in agreement with other studies[46, 47]. Singh A et al [48] reported that, NAB-SAL diminished tumor growth, induces cell cycle arrest and apoptosis in OSCC cells, resulting in antiproliferative effects in vitro and in vivo: in a mouse model, significant growth inhibition of the OSCC tumor was observed.

The IHC staining of GIII using CD44 antibody showed positive membranous expression (mean= 49.07 %) throughout the epithelial layers and invading tumor cells, that showed highly significantly expression compared to GII (p value < 0.001) CD44 down-regulation indicates NAB-SAL could inhibit CSCs or induce CSCs transforming, which is one key target for suppression of tumor progression. These results agree with that of other investigators **[49-51]**. Wang Q et al [52] found that, Co-delivery of SAL with NAB decreased CD44 expression, suggesting that NAB-SAL exerted the strongest inhibition efficacy of CSCs.

5 Conclusion

NAB-SAL significantly inhibits tumor progression through direct influence on CSCs of DMBA induced HBP carcinoma. targeted NAB-SAL makes an important and useful novel effective agent against CSCs. Furthermore, the approval of antibiotics as an effective agent against CSCs modality in the treatment of OSSC has started a new era in combinatorial therapeutic approaches for this disease. Further investigations need to appreciate both the benefits and the risks posed by inhibiting these alternative therapeutic pathways and ultimately how they impact the tumor microenvironment.

6. References

1. Ezhilarasan D, Lakshmi T, Subha M, Deepak Nallasamy V, Raghunandhakumar SJOD. The ambiguous role of sirtuins in head and neck squamous cell carcinoma. 2022;28(3):559-67.
2. Martínez B DA, Barato Gómez PA, Iregui Castro CA, Rosas Pérez JEJBRI. DMBA-induced oral carcinoma in Syrian hamster: increased carcinogenic effect by dexamethasone coexposition. 2020;2020.
3. Li S, Xu S, Liang X, Xue Y, Mei J, Ma Y, et al. Nanotechnology: breaking the current treatment limits of lung cancer. 2021;10(12):2100078.
4. Cheng B, Yang G, Jiang R, Cheng Y, Yang H, Pei L, et al. Cancer stem cell markers predict a poor prognosis in renal cell carcinoma: a meta-analysis. 2016;7(40):65862.
5. Gao Y, Shang Q, Li W, Guo W, Stojadinovic A, Mannion C, et al. Antibiotics for cancer treatment: A double-edged sword. 2020;11(17):5135.
6. Alsaadi M, Tezcan G, Garanina EE, Hamza S, McIntyre A, Rizvanov AA, et al. Doxycycline attenuates cancer cell growth by suppressing NLRP3-mediated inflammation. 2021;14(9):852.
7. Dembitsky VMJMD. Natural polyether ionophores and their pharmacological profile. 2022;20(5):292.
8. Ester K, Mioč M, Spurny P, Bonhenry D, Marjanović M, Uzelac L, et al. Targeting plasma membrane and mitochondrial instability in breast cancer cells and breast epithelial to mesenchymal transition-model cells by adamantyl diaza-crown ether ZG613. 2022:2022.09. 30.510273.
9. Fuchs D, Heinold A, Opelz G, Daniel V, Naujokat CJB, communications br. Salinomycin induces apoptosis and overcomes apoptosis resistance in human cancer cells. 2009;390(3):743-9.
10. Wang H, Zhang H, Zhu Y, Wu Z, Cui C, Cai FJFiO. Anticancer mechanisms of salinomycin in breast cancer and its clinical applications. 2021;11:654428.
11. Khwaza V, Mbese Z, Aderibigbe BA, Oyedeji OO. Therapeutic Efficacy of Antibiotics in the Treatment of Chronic Diseases. Antibiotic Materials in Healthcare: Elsevier; 2020. p. 11-32.
12. Lo Muzio L, Sartini D, Santarelli A, Rocchetti R, Morganti S, Pozzi V, et al. Expression and prognostic significance of apoptotic genes in oral squamous cell carcinoma. Molecular carcinogenesis. 2014;53(4):264-71.
13. Bose P, Klimowicz AC, Kornaga E, Petrillo SK, Matthews TW, Chandarana S, et al. Bax expression measured by AQUAnalysis is an independent prognostic marker in oral squamous cell carcinoma. BMC cancer. 2012;12(1):332.
14. Tewabe A, Abate A, Tamrie M, Seyfu A, Abdela Siraj EJJoMH. Targeted drug delivery—from magic bullet to nanomedicine: principles, challenges, and future perspectives. 2021:1711-24.
15. Scaranti M, Cojocaru E, Banerjee S, Banerji UJNrco. Exploiting the folate receptor α in oncology. 2020;17(6):349-59.
16. Saleh MM, Darwish ZE, El Nouaem MI, Mourad GM, Ramadan ORJADJ. Chemopreventive effect of green tea and curcumin in induced oral squamous cell carcinoma: An experimental study. 2020;45(3):74-80.
17. Zhou J, Sun J, Chen H, Peng QJIJoO. Promoted delivery of salinomycin sodium to lung cancer cells by dual targeting PLGA hybrid nanoparticles. 2018;53(3):1289-300.
18. Al-Dosoki MA A-AA, Omar AMZ, Zouair MGA. Flow cytometric assessment of nivolumab and/or epigallocatechin-3-gallate on cancer stem cells of DMBA induced hamster buccal pouch carcinoma. Medical Science. 2021;25(118):3206-21.
19. Faisal M, Abu Bakar M, Sarwar A, Adeel M, Batool F, Malik KI, et al. Depth of invasion (DOI) as a predictor of cervical nodal metastasis and local recurrence in early stage squamous cell carcinoma of oral tongue (ESSCOT). PloS one. 2018;13(8):e0202632.
20. Kim S-W, Roh J, Park C-SJJop, medicine t. Immunohistochemistry for pathologists: protocols, pitfalls, and tips. 2016;50(6):411-8.

21. Patil K, Khan FB, Akhtar S, Ahmad A, Uddin SJC, Reviews M. The plasticity of pancreatic cancer stem cells: Implications in therapeutic resistance. 2021;40(3):691-720.
22. Bruna F, Arango-Rodríguez M, Plaza A, Espinoza I, Conget PJScr. The administration of multipotent stromal cells at precancerous stage precludes tumor growth and epithelial dedifferentiation of oral squamous cell carcinoma. 2017;18:5-13.
23. El-Hossary WH, Hegazy E, El-Mansy MNJEDJ. Topical chemopreventive effect of thymoquinone versus thymoquinone loaded on gold nanoparticles on DMBA-induced hamster buccal pouch carcinogenesis (immunohistochemical study). 2018;64(4-October (Oral Medicine, X-Ray, Oral Biology & Oral Pathology)):3523-33.
24. A Al-Dosoki M, M Mansour A, M Ahmed MJA-AJoDS. Effect of oxygenated water as a new treatment modality on experimentally induced hamster buccal pouch carcinogenesis. 2018;21(3):261-73.
25. Krishna Prasad R. Expression of Cyclin D1 in Normal Oral Mucosa, Epithelial Dysplasia and Oral Squamous Cell Carcinoma: Sree Mookambika Institute of Denal Sciences, Kulasekharam; 2016.
26. Singh R, Letai A, Sarosiek KJNrMcb. Regulation of apoptosis in health and disease: the balancing act of BCL-2 family proteins. 2019;20(3):175-93.
27. Kaza S, Kantheti LP, Poosarla C, Gontu SR, Kattappagari KK, Baddam VRJJoOS. A study on the expression of CD44 adhesion molecule in oral squamous cell carcinoma and its correlation with tumor histological grading. 2018;10(1):42.
28. French R, Pauklin SJIJoC. Epigenetic regulation of cancer stem cell formation and maintenance. 2021;148(12):2884-97.
29. Aquib A, Yadav AK. CD44 alternative splice variants v6 and v10. 2020.
30. El-Mansy MN, Hassan MM, El-Nour A, Kholoud M, El-Hosary WHJSCUMJ. Treatment of oral squamous cell carcinoma using thymoquinone loaded on gold nanoparticles. 2017;20(1):11-9.
31. Sophia J, Kiran Kishore T K, Kowshik J, Mishra R, Nagini SJSr. Nimbolide, a neem limonoid inhibits Phosphatidyl Inositol-3 Kinase to activate Glycogen Synthase Kinase-3β in a hamster model of oral oncogenesis. 2016;6(1):1-13.
32. Manoharan S, Rajasekaran D, Prabhakar MM, Karthikeyan S, Manimaran AJTi. Modulating effect of Enicostemma littorale on the expression pattern of apoptotic, cell proliferative, inflammatory and angiogenic markers during 7, 12-dimethylbenz (a) anthracene induced hamster buccal pouch carcinogenesis. 2015;22(1):130.
33. Suhail N, Bilal N, Hasan S, Ahmad A, Ashraf GM, Banu NJCS, et al. Chronic unpredictable stress (CUS) enhances the carcinogenic potential of 7, 12-dimethylbenz (a) anthracene (DMBA) and accelerates the onset of tumor development in Swiss albino mice. 2015;20:1023-36.
34. Arfin S, Jha NK, Jha SK, Kesari KK, Ruokolainen J, Roychoudhury S, et al. Oxidative stress in cancer cell metabolism. 2021;10(5):642.
35. Pallavi N, Nalabolu GRK, Hiremath SKSJJoO, JOMFP MP. Bcl-2 and c-Myc expression in oral dysplasia and oral squamous cell carcinoma: An immunohistochemical study to assess tumor progression. 2018;22(3):325.
36. Juneja S, Chaitanya NB, Agarwal MJIjoc. Immunohistochemical expression of Bcl-2 in oral epithelial dysplasia and oral squamous cell carcinoma. 2015;52(4):505-10.
37. Singh L, Pushker N, Saini N, Sen S, Sharma A, Bakhshi S, et al. Expression of pro-apoptotic Bax and anti-apoptotic Bcl-2 proteins in human retinoblastoma. 2015;43(3):259-67.
38. Maheswari U. Expression of Annexin Al and KI-67 in histopathologically negative margins of oral squamous cell carcinoma cases with and without local recurrence: Vivekanandha Dental College for Women, Tiruchengode; 2018.
39. Stewart RL. Clinical and Pathologic Significance of Integrin A6β4 Expression in Human Malignancies. 2015.
40. Mirhashemi M, Ghazi N, Saghravanian N, Taghipour A, Mohajertehran FJDRJ. Evaluation of CD24 and CD44 as cancer stem cell markers in squamous cell carcinoma and epithelial dysplasia of the oral cavity by q-RT-PCR. 2020;17(3):208.
41. Kashyap T, Pramanik KK, Nath N, Mishra P, Singh AK, Nagini S, et al. Crosstalk between Raf-MEK-ERK and PI3K-Akt-GSK3β signaling networks promotes chemoresistance, invasion/migration and stemness via expression of CD44 variants (v4 and v6) in oral cancer. 2018;86:234-43.

42. Tamatani T, Takamaru N, Ohe G, Akita K, Nakagawa T, Miyamoto YJOl. Expression of CD44, CD44v9, ABCG2, CD24, Bmi-1 and ALDH1 in stage I and II oral squamous cell carcinoma and their association with clinicopathological factors. 2018;16(1):1133-40.
43. Paulis YW, Huijbers EJ, van der Schaft DW, Soetekouw PM, Pauwels P, Tjan-Heijnen VC, et al. CD44 enhances tumor aggressiveness by promoting tumor cell plasticity. Oncotarget. 2015;6(23):19634.
44. Mărgăritescu C, Pirici D, Simionescu C, Stepan A. The utility of CD44, CD117 and CD133 in identification of cancer stem cells (CSC) in oral squamous cell carcinomas (OSCC). Rom J Morphol Embryol. 2011;52(3 Suppl):985-93.
45. Paik ES, Kim T-H, Cho YJ, Ryu J, Choi J-J, Lee Y-Y, et al. Preclinical assessment of the VEGFR inhibitor axitinib as a therapeutic agent for epithelial ovarian cancer. Scientific reports. 2020;10(1):1-9.
46. Benvenuto M, Albonici L, Focaccetti C, Ciuffa S, Fazi S, Cifaldi L, et al. Polyphenol-mediated autophagy in cancer: evidence of in vitro and in vivo studies. 2020;21(18):6635.
47. Antoszczak M, Huczyński AJA-CAiMC. Anticancer activity of polyether ionophore-salinomycin. 2015;15(5):575-91.
48. Singh AK, Verma A, Singh A, Arya RK, Maheshwari S, Chaturvedi P, et al. Salinomycin inhibits epigenetic modulator EZH2 to enhance death receptors in colon cancer stem cells. 2021;16(2):144-61.
49. Tian L, Goldstein A, Wang H, Ching Lo H, Sun Kim I, Welte T, et al. Mutual regulation of tumour vessel normalization and immunostimulatory reprogramming. Nature. 2017;544(7649):250-4.
50. Zheng X, Fang Z, Liu X, Deng S, Zhou P, Wang X, et al. Increased vessel perfusion predicts the efficacy of immune checkpoint blockade. The Journal of clinical investigation. 2018;128(5):2104-15.
51. Swiecicki PL, Zhao L, Belile E, Sacco AG, Chepeha DB, Dobrosotskaya I, et al. A phase II study evaluating axitinib in patients with unresectable, recurrent or metastatic head and neck cancer. 2015;33:1248-56.
52. Wang Q, Yen Y-T, Xie C, Liu F, Liu Q, Wei J, et al. Combined delivery of salinomycin and docetaxel by dual-targeting gelatinase nanoparticles effectively inhibits cervical cancer cells and cancer stem cells. 2021;28(1):510-9.